EXTREME ULTRAVIOLET-LASER SPECTROSCOPY ON CO IN THE 91-100 NM RANGE

Levelt, P.F.; Ubachs, W.M.G.; Hogervorst, W.

published in
Journal of Chemical Physics
1992

DOI (link to publisher)
10.1063/1.463540

document version
Publisher's PDF, also known as Version of record

Extreme ultraviolet laser spectroscopy on CO in the 91–100 nm range

Pieternel F. Levelt, Wim Ubachs, and Wim Hogervorst
Laser Centre Free University, Department of Physics and Astronomy, De Boelelaan 1081, 1081 HV Amsterdam, The Netherlands

(Received 8 June 1992; accepted 10 August 1992)

Transitions from the ground state $X\,^1\Sigma^+$ $v=0$ to eleven highly-excited states of CO were investigated using extreme ultraviolet laser spectroscopy. Excited states were detected using a two-photon ionization scheme. Improved values of band origins could be deduced from an absolute calibration of the extreme ultraviolet laser radiation against the I_2 standard in the visible wavelength region. Accurate predissociation rates followed from linewidth analyses of individual rotational lines.

I. INTRODUCTION

In recent years the absorption spectrum of carbon monoxide in the extreme ultraviolet (XUV) wavelength range has attracted renewed interest because new and advanced equipment for high resolution investigations became available. Large classical spectrometers such as the 10 m VUV spectrograph of Meudon,[1,2] synchrotron radiation sources such as the KEK photon factory in Japan[3,4] and laser-based tunable XUV sources[5] now offer an instrumental bandwidth of ~ 0.5 cm^{-1}, i.e., a resolving power of 2×10^5. This continued research is mainly motivated by the demand for accurate values on spectral line positions, absorption cross sections and photodissociation rates to be used in chemical models for molecular clouds existing in various regions of outer space.[6,7]

A vibrationally-resolved absorption spectrum recorded with synchrotron radiation provides an overview of the astrophysically relevant range 88.5–115 nm.[8] These measurements yielded first reliable values for absorption cross sections and photodissociation rates for 46 distinguishable vibronic features. As an important result it was established that the XUV-induced photodestruction of CO occurs predominantly via discrete line-absorption. The quest is now for rotational resolution and for individual line-dependent parameters governing the photodynamics of CO. A comprehensive study of the range 91.2–115.2, including different isotopes of CO, was reported by Eidelsberg *et al.*[1,2] using the spectrograph of Meudon.

In addition to the straightforward use of XUV-photons, highly excited states of CO can also be probed in multiphoton schemes. Hines *et al.*[9] applied a 2+1 single color REMPI-scheme for a study of the $E\,^1\Pi$, $v=0$ state. In multistep two[10] and three[11] color resonant schemes single rotational quantum states could be elegantly prepared before the final excitation of the Rydberg state. Finally, optogalvanic studies have been performed.[12,13] They have the experimental advantage that highly-excited states in the CO-molecule can be investigated with a single visible photon. The multiphoton and optogalvanic laser schemes have in common that they do not provide information on XUV absorption cross sections; nevertheless the spectroscopic information obtained on highly-excited states is useful and may in principle be as accurate as information deduced from direct XUV-excitation.

The mechanism(s) leading to predissociation of the excited states in the range above the dissociation limit ($89\,592\pm 15$ cm^{-1} above the $X\,^1\Sigma^+$ $v=0$, $J=0$ ground state of CO) are not yet understood. As an exception predissociation in the $B\ (3s\sigma)\,^1\Sigma^+$ Rydberg states, for $v=1$ $J\geqslant 36$ and $v=2$, all J, was found to be caused by the $D'\,^1\Sigma^+$ valence state.[14] To attain a complete understanding of the predissociation processes involving states in the important energy range 89 000–110 000 cm^{-1}, combined efforts of experimentalists and theoreticians are still needed.

In a program to remeasure and improve upon the existing spectroscopic data on CO in the wavelength range 91–100 nm we recorded spectra of 11 vibronic bands using our newly-built XUV-laser spectrometer. In a preliminary report[5] data on two of these bands were already presented in detail. In the present paper accurate spectroscopic data as well as predissociation rates on nine vibronic states (the two remaining bands were too weak to extract useful spectroscopic information) in the energy range 100 000–110 000 cm^{-1} are reported; two vibrational states $v=0$ and 2 of the lowest Rydberg state $W\ (3s\sigma)\,^1\Pi$ converging to the $A\,^2\Pi$ ion core, several Rydberg states converging to the $X\,^2\Sigma^+$ core, $(5p\sigma)\,^1\Sigma^+$ $v=1$, $L\ (4p\pi)\,^1\Pi$ $v=0$, $K\ (4p\sigma)\,^1\Sigma^+$ $v=0$, $(4d\sigma)\,^1\Sigma^+$ $v=0$, $L'(3d\pi)\,^1\Pi$ $v=1$, and two more states of $^1\Sigma^+$ and $^1\Pi$ symmetry which are not yet spectroscopically identified in terms of molecular orbitals.

II. EXPERIMENT

A concise description of the XUV-laser spectrometer was given in a previous paper.[5] Here we give only some relevant experimental details. CO molecules are excited under collision-free circumstances in a pulsed molecular beam expansion. Depending on time-delay settings either a cold (~ 40 K) or an almost room temperature (~ 250 K) rotational population distribution is probed by the pulsed (5 ns) XUV-light in a crossed-beam configuration. In this setup the Doppler contribution to the experimental linewidth is <0.02 cm^{-1}. The XUV-radiation is the exact sixth harmonic of a tunable dye laser at visible frequencies and is generated in two stages, frequency doubling of the fundamental in a crystal followed by frequency tripling of the UV laser light in a rare-gas medium. The XUV-beam diverges into the interaction zone where the molecules experience an XUV power density at the peak of the pulse of ~ 1 W/cm^2. An UV-pulse temporally and spatially overlaps the XUV-laser pulse ($\lambda_{UV}=3\lambda_{XUV}$) with a peak

 0021-9606/92/227160-07$006.00

power of ~ 3 MW/cm^2. CO molecules, excited by resonant XUV photons are subsequently ionized by this UV-light. The CO-ions are mass-selected before detection by means of a time-of-flight set-up allowing the recording of independent ^{12}CO and ^{13}CO spectra from a natural CO sample.

The spectral width of the XUV radiation was found to depend on alignment, pumping rate, and dye-concentration in the oscillator stage of the laser at the fundamental frequency. The instrumental width is predominantly determined by this XUV-linewidth. Selected transitions in molecular nitrogen [$b'\,^1\Sigma_u^+$, $v=1$ (Ref. 15) and $v=7$] and fluorine ($H\,^1\Pi_u$ $v=0$ and $v=1$) were recorded, also by means of 1 XUV+1 UV resonance ionization. The estimated predissociation rates for these excited states of N_2 and F_2 preclude observable line broadening at the present level of resolution. From detailed analysis of the line profiles of a number of resonances in the N_2 and F_2 spectra we find that (i) the line profiles are of Gaussian shape, and (ii) the width at full-width half-maximum (FWHM) is 0.32 ± 0.06 cm^{-1}. This value, somewhat lower than a previous estimate,[5] but consistent within the estimated error bars, is taken as the instrumental bandwidth of the XUV laser spectrometer.

The simultaneous recording of an I_2-absorption spectrum in the visible with a CO-excitation spectrum in the XUV range provides an elegant tool for absolute frequency calibration. Based on the assumption of harmonic locking of the XUV and fundamental frequencies, line positions of CO resonances were accurately determined on an absolute frequency scale using a computerized interpolation method. The absolute accuracy of the I_2 reference spectrum[16,17] is 0.002 cm^{-1}. The spectral width of the fundamental radiation (~ 0.07 cm^{-1}) however limits the accuracy in the reference lines to ~ 0.015 cm^{-1}. Line positions of strong and unblended CO resonances can be determined to 10% of the observable widths, i.e., with a relative accuracy of about ~ 0.04 cm^{-1}. The absolute accuracy in the frequency positions of CO-lines is therefore estimated at 0.13 cm^{-1} ($=6\times 0.015$ cm$^{-1}+0.04$ cm^{-1}).

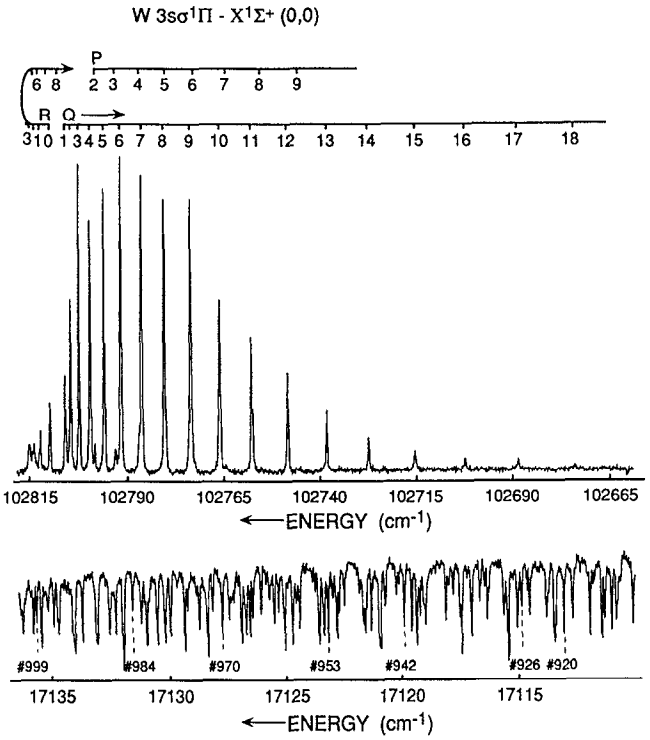

FIG. 1. (Upper part) 1 XUV+1 UV resonance-enhanced two-photon ionization spectrum of the $W\,(3s\sigma)^1\Pi$–$X\,^1\Sigma^+$ (0,0) transition in ^{12}CO at 97.27 nm observed in a molecular beam of near room temperature rotational distribution. R, P, and Q-branches are identified. (Lower part) I_2-absorption spectrum recorded in the visible wavelength region. Some of the unblended and symmetrical I_2-lines used for the calibration are marked with (#). Reference is made to numbers in the I_2-atlas.

III. RESULTS

Resonance ionization (1 XUV+1 UV) spectra of CO were recorded in the wavelength range 91–100 nm with the XUV laser spectrometer. Eleven vibronic bands were observed in excitation from the $X\,^1\Sigma^+$, $v=0$ ground state. Nine of these were intense enough to identify rotationally resolved lines and to extract spectroscopic information. Eidelsberg *et al.*,[1,2] in direct absorption studies in the same energy range, identified 37 different vibronic features. The analysis of two strong transitions to the $K\,(4p\sigma)^1\Sigma^+$ $v=0$ and $W\,(3s\sigma)^1\Pi$ $v=2$ states at 97.04 and 94.12 nm was presented in a previous paper.[5] In the present paper results of XUV-laser studies on seven additional excited states will be reported. The spectroscopic identification of Eidelsberg *et al.*[1,2] will be followed throughout this paper. In this annotation the $W\,(3s\sigma)^1\Pi$ $v=0$, the $(5p\sigma)^1\Sigma^+$ $v=1$, a $^1\Sigma^+$ $v=2$, and the $L\,(4p\pi)^1\Pi$ $v=0$ states were recorded in strong transitions with band origins at 97.27, 91.34, 91.37, and 96.83 nm, respectively. All four bands were measured at least six times in molecular beams with hot and cold population distributions, showing high-J and low-J rotational lines in separate spectra. In Figs. 1–3 recordings of these four bands are shown. The $L'\,(3d\pi)^1\Pi$ $v=1$ and $(4d\sigma)^1\Sigma^+$ $v=0$ states and a $^1\Pi$ $v=2$ state, at 96.89, 94.63, and 92.87 nm, respectively, could only be observed as weak features in cooled expansions. Two other extremely weak features belonging to the $^1\Pi$–$X\,^1\Sigma^+$ (0,0) and $(6p\sigma)^1\Sigma^+$–$X\,^1\Sigma^+$ (0,0) transitions at, respectively, 91.27 and 91.60 nm, were recorded at a low signal to noise ratio and no reliable spectroscopic information was inferred. In the supersonically-cooled part of the molecular beam expansion of pure and natural CO (1% ^{13}CO) with a dense population of J states, a spectrum of the strong W–X (0,0) band of ^{13}CO could be recorded as well near 97.30 nm.

A. Spectroscopy

The transition frequencies of resolved rotational lines in seven bands were compared with expressions for $^1\Sigma$–$^1\Sigma$ and $^1\Pi$–$^1\Sigma$ transitions,

$$\nu=\nu_0+BJ(J+1)-DJ^2(J+1)^2-E_g(J''), \qquad (1)$$

where ν_0 is the band origin, B is the rotational constant, D is the centrifugal distortion constant, and J is the rotational quantum number of the excited vibronic state. The ground-state energy levels $E_g(J'')$ were calculated from spectroscopic constants of Guelachvili *et al.*[18] The average transi-

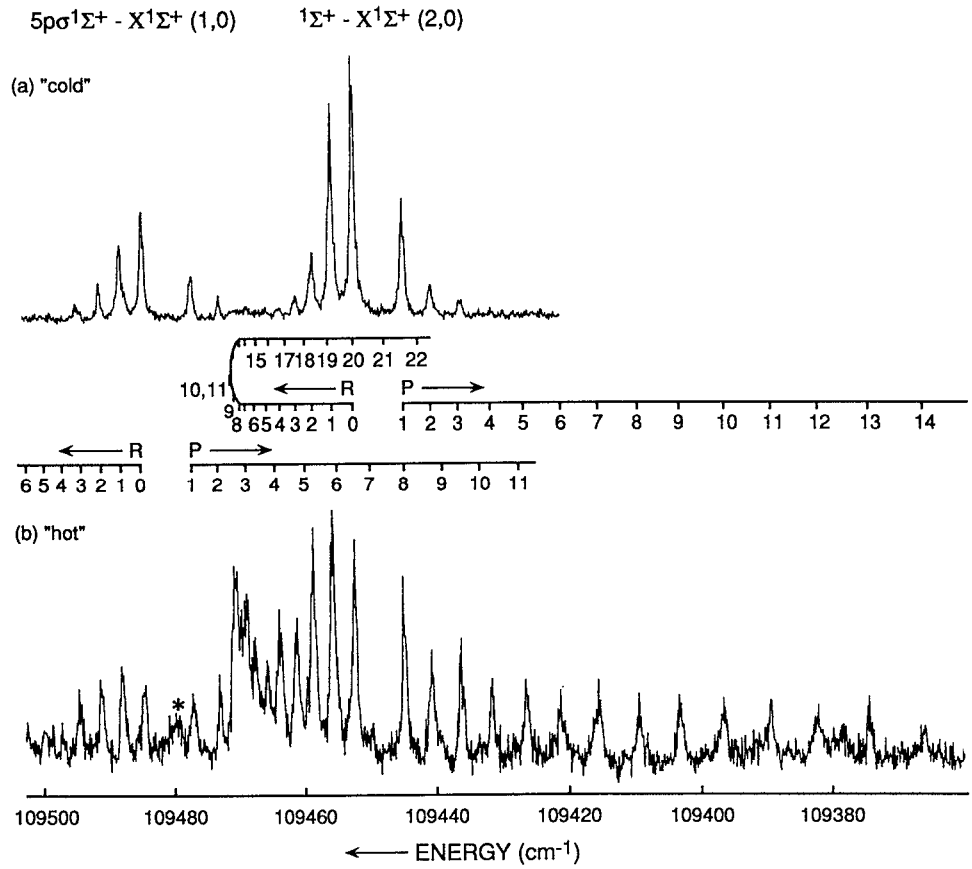

FIG. 2. XUV excitation spectrum of the $(5p\sigma)^1\Sigma^+$–$X\,^1\Sigma^+$ (1,0) and $^1\Sigma^+$–$X\,^1\Sigma^+$ (2,0) bands at 91.34 and 91.37 nm observed in a cold beam of ^{12}CO (a) and in a molecular beam of 250 K (b). The broad feature indicated with (*) is the Q-bandhead of a $(5p\pi)^1\Pi$–$X\,^1\Sigma^+$ (1,0) transition (Ref. 2).

tion frequencies and uncertainties are listed in Tables I–VI for six different bands. The frequency scales of the spectra were linearized by fitting a spline function through a manifold of iodine lines. The I_2– and XUV-resonances were fitted with Gaussian and Voigt profiles. The CO resonance frequencies were determined by computerized interpolation between selected I_2 lines, multiplying the resulting frequency with a factor of 6. The spectroscopic constants were determined by fitting the experimental data to the calculated transition frequencies in a least-squares minimization routine. As information on high J-states obtained in the present experiment is rather limited and the resolution in the spectra is only slightly better than in the spectra recorded by Eidelsberg *et al.*[1,2] we do not expect a significant improvement in the accuracy of rotational constants. Therefore apart from a few cases, we kept the rotational constants B and D fixed at Eidelsberg's values and focused attention on a determination of accurate band origins ν_0. Here full advantage is taken of the absolute calibration accuracy of the XUV laser spectrometer. The resulting spectroscopic constants are listed in Table VII. The spectroscopic constants for the K $(4p\sigma)^1\Sigma^+$ $v=0$ and W $(3s\sigma)^1\Pi$ $v=2$ states, published earlier,[5] are also included for reasons of completeness.

For a description of the L $(4p\pi)^1\Pi$–$X\,^1\Sigma_g^+$ $v=0$ transition it turned out to be necessary to include Λ-doubling, i.e., a splitting in a Π^+ level, probed in the P and R

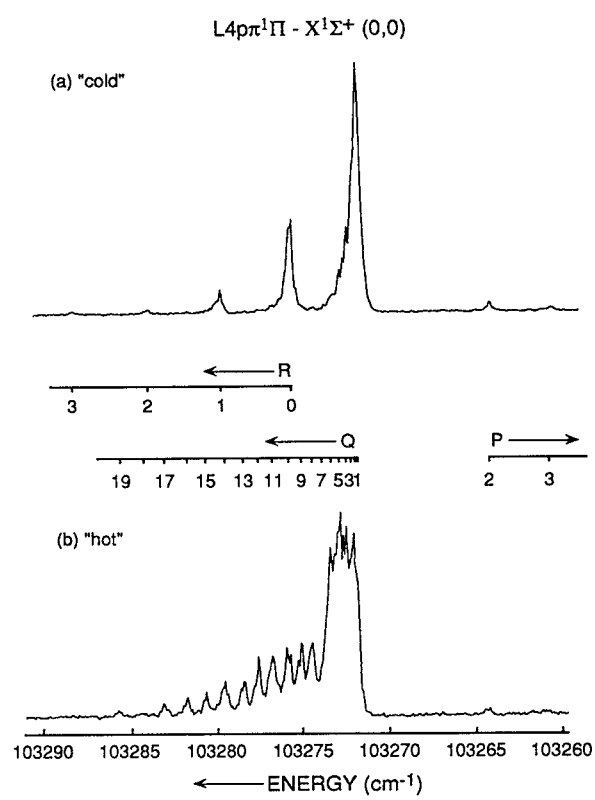

FIG. 3. "Cold" (a) and "hot" (b) spectrum of the L $(4p\pi)^1\Pi$–$X\,^1\Sigma^+$ (0,0) transition at 96.83 nm.

TABLE I. Observed line positions in the $W\,^1\Pi$–$X\,^1\Sigma^+$ (0,0) band at 97.27 nm for ^{12}CO and at 97.30 nm for ^{13}CO (with *). Differences between observed and calculated line positions [with formula (1)] are also included. Lines marked with (a) were not used in the minimization routine because of large uncertainties. Lines marked with (b) are blended. All values are in cm^{-1}.

	$R(J)$		$Q(J)$		$P(J)$	
J	observed	obs.−calc.	observed	obs.−calc.	observed	obs.−calc.
0	102 809.88(5)	0.02				
0	*102 778.70(5)	−0.02				
1	102 812.35(6)	0.08	102 805.98(4)	−0.04		
1	*102 781.09(5)	0.05	*102 775.03(5)	−0.01		
2	102 813.85(8)	−0.10	102 804.51(5)	−0.07	102 798.24(10)	−0.09
2			*102 773.61(5)	−0.08		
3			102 802.42(8)	0.00	102 793.07(10)	0.02
3			*102 771.73(6)	0.07		
4			102 799.50(9)	−0.02		
5			102 795.95(9)	0.06		
6			102 791.61(4)	0.09		
7			102 786.37(7)(b)	−0.01		
8			102 780.47(6)(b)	−0.01		
9			102 773.78(7)	−0.01		
10			102 766.32(7)	0.02		
11			102 758.05(6)	0.05		
12			102 748.87(6)	0.02		
13			102 738.76(6)	−0.08		
14			102 727.80(8)	−0.14		
15			102 716.08(8)	−0.05		
16			102 703.40(9)	0.02		
17			102 689.79(9)	0.12		
18			102 675.54(a)			

branches, and a Π^- level probed in the Q lines. In that case the transition frequencies to Π^+ and Π^- states were equated with

$$\nu_{\Pi^+} = \nu_0 + BJ(J+1) - DJ^2(J+1)^2 + q_\Pi J(J+1) - E_g(J''),$$
$$\nu_{\Pi^-} = \nu_0 + BJ(J+1) - DJ^2(J+1)^2 - E_g(J''), \quad (2)$$

where q_Π is the Λ-doubling parameter. Even with the inclusion of Λ-doubling the assignment of Q-lines in the L $(4p\pi)\,^1\Pi$–$X\,^1\Sigma^+$ (0,0) band at 96.83 nm turned out to be far from trivial. Also the data in the CO-atlas[2] were of no guidance; the reported data for this Q-branch did not match the present observations. However a consistent assignment was found by making use of accurate spectroscopic constants for the $L\,^1\Pi$ state (including Λ-doubling) determined by optogalvanic spectroscopy[12] as well as choosing the first individual rotational line at the high-frequency side of the congested Q-bandhead to be the $Q(8)$ line. With this identification the strong dip in intensity between the $Q(8)$ line and the Q-bandhead (see Fig. 3) reflects an anomalously weak $Q(7)$ transition. The same effect was found even more pronounced in the optogalvanic experiment.[12] It was attributed to an accidental predissociation of the Π^- component of the $J=7$ level.

TABLE II. Observed line positions in the $^1\Sigma^+$–$X\,^1\Sigma^+$ (2,0) band for ^{12}CO at 91.37 nm. Differences between observed and calculated line positions [with formula (1)] are also included. All values are in cm^{-1}.

	$R(J)$		$P(J)$	
J	observed	obs.−calc.	observed	obs.−calc.
0	109 452.48(7)	−0.04		
1	109 455.79(9)	0.00	109 445.02(7)	−0.10
2	109 458.72(9)	−0.04	109 440.80(12)	−0.19
3	109 461.27(12)	−0.17	109 436.46(12)	−0.10
4	109 463.86(14)	0.05	109 431.98(7)	0.13
5			109 426.91(7)	0.07
6			109 421.78(10)	0.25
7			109 415.96(10)	0.05
8			109 409.93(10)	−0.05
9			109 403.67(15)	−0.06
10			109 397.31(15)	0.16
11			109 390.29(20)	0.06
12			109 382.93(2)	−0.04
13			109 375.16(20)	−0.17
14			109 366.92(30)	−0.40

B. Predissociation

Varying widths were observed for individually resolved rotational lines in the different CO bands. The spectral width in the transition to the L $(4p\pi)\,^1\Pi$ $v=0$ band equals

TABLE III. Observed line positions in the $(5p\sigma)\,^1\Sigma^+$–$X\,^1\Sigma^+$ (1,0) band for ^{12}CO at 91.34 nm. Differences between observed and calculated line positions [with formula (1)] are also included. All values are in cm^{-1}.

	$R(J)$		$P(J)$	
J	observed	obs.−calc.	observed	obs.−calc.
0	109 484.72(4)	0.03		
1	109 488.11(6)	−0.05	109 477.29(8)	0.10
2	109 491.34(8)	−0.10	109 473.17(8)	0.02
3	109 494.60(8)	0.06		
4	109 497.12(15)	−0.32		

TABLE IV. Observed line positions in the $L\ (4p\pi)^1\Pi$–$X\ ^1\Sigma^+$ (0,0) band for ^{12}CO at 96.83 nm. Differences between observed and calculated line positions [with formula (2)] are also included. Lines marked with (b) are blended. All values are in cm^{-1}.

	$R(J)$		$Q(J)$		$P(J)$	
J	observed	obs.−calc.	observed	obs.−calc.	observed	obs.−calc.
0	103 275.86(10)	0.03				
1	103 279.92(4)	0.01				
2	103 284.12(4)	0.01			103 264.25(7)	−0.05
3	103 288.44(6)	0.02			103 260.72(4)	0.03
4					103 257.17(5)	−0.03
5					103 253.92(5)	0.10
8			103 274.52(4)	−0.02		
9			103 275.18(5)	−0.03		
10			103 275.93(7)(b)	−0.02		
11			103 276.80(4)	0.03		
12			103 277.65(4)	0.00		
13			103 278.56(4)	−0.06		
14			103 279.68(5)(b)	0.03		
15			103 280.74(4)	−0.02		
16			103 281.91(4)	−0.03		
17			103 283.25(5)	0.06		
19			103 285.85(5)	−0.06		

the estimated instrumental linewidth, while the linewidths in the $L'\ (3d\pi)^1\Pi$–$X\ ^1\Sigma^+$ (1,0) spectrum are up to 1.5 cm^{-1}. The line-broadening may be attributed to predissociation of the excited levels. The observed linewidth $\delta\nu_{obs}$ is a convolution of instrumental linewidth $\delta\nu_{instr}$ (of Gaussian shape) and the linewidth Γ caused by predissociation (Lorentzian profile). To estimate the intrinsic linewidth Γ the following analytical deconvolution of a Voigt profile is used[19]:

$$\Gamma=\delta\nu_{obs}-(\delta\nu_{instr})^2/\delta\nu_{obs} \tag{3}$$

which is valid under the condition that $\delta\nu_{instr}$ is of Gaussian and Γ of Lorentzian line shape. Lifetime τ and intrinsic linewidth Γ are related by

$$k_p=\tau^{-1}=2\pi\,\Gamma c, \tag{4}$$

where c is the speed of light and k_p is the predissociation rate. Here it is assumed that radiative relaxation is a much slower process than predissociation; the excited CO levels are indeed known to effectively predissociate for 99%.[2,8] It should be noted that residual Doppler broadening is included in the instrumental linewidth.

The observed shapes of unblended lines were fitted with a Voigt-profile and good agreement was found between the synthetic and observed line shapes. From this procedure accurate values $\delta\nu_{obs}$ for the experimental widths (FWHM) were determined. Using the deconvolution procedure of Eq. (3) with $\delta\nu_{instr}=0.32\pm0.06$ cm^{-1} predissociation rates and lifetimes are derived. Values for the different states under investigation are listed in Table VIII. We verified that various possible saturation mechanisms, such as power broadening and ionization depletion, which might give rise to additional line broadening, did not affect our results. Also included in Table VIII are improved values for predissociation rates for the $K\ (4p\sigma)^1\Sigma^+$ $v=0$ and $W\ (3s\sigma)^1\Pi$ $v=2$ states. The intrinsic linewidths were now deduced in a way that differs in two respects from the preliminary analysis reported in Ref. 5. First, a fit with a Voigt function was implemented, resulting in better agreement with the observed line profile as with the earlier used Gaussian function. Second, the new value of 0.32 ±0.06 cm^{-1} for the instrumental linewidth was used in the deconvolution procedure of Eq. (3).

Important for an implementation of predissociation effects in models for the interstellar medium are dependencies of predissociation rates on rotational states. We did not observe any systematic variation in the linewidths for rotational states within a particular band, however with one exception. Notwithstanding the low signal to noise ratio some indication of a rotational-state-dependent line broadening in the $^1\Pi$–$X\ ^1\Sigma^+$ (2,0) band at 92.87 nm was

TABLE V. Observed line positions in the $(4d\sigma)^1\Sigma^+$–$X\ ^1\Sigma^+$ (0,0) band for ^{12}CO at 94.63 nm. Differences between observed and calculated line positions [with formula (1)] are also included. All values are in cm^{-1}.

	$R(J)$		$P(J)$	
J	observed	obs.−calc.	observed	obs.−calc.
0	105 680.22(8)	−0.05		
1	105 684.02(10)	+0.06	105 672.58(10)	−0.08
2	105 687.69(10)	+0.12	105 668.73(10)	−0.01

TABLE VI. Observed line positions in the $^1\Pi$–$X\ ^1\Sigma^+$ (2,0) band for ^{12}CO at 92.87 nm. Differences between observed and calculated line positions [with formula (1)] are also included. The Q-bandhead (a) was not included in the minimization routine. All values are in cm^{-1}.

	$R(J)$		Q-head
J	observed	obs.−calc.	observed
0	107 685.71(6)	−0.08	
1	107 689.65(6)	+0.06	107 681.78(a)
2	107 693.40(6)	+0.03	

TABLE VII. Spectroscopic constants for several states of ^{12}CO and ^{13}CO. Values marked with (a) were taken from Eidelsberg *et al.* (Refs. 1 and 2) and with (b) from Sekine *et al.* (Ref. 12) and fixed in the minimization routine. $\delta\nu_0$ represents the difference between the present value for the band origin and the value given in Ref. 2. The values for the bands indicated with (c) were already published in a perliminary report (Ref. 5). It should be noted that our estimate for the absolute frequency uncertainty in the band origins ν_0 is 0.13 cm^{-1}.

		ν_0 (cm^{-1})	B (cm^{-1})	D (cm^{-1})	q_π (cm^{-1})	$\delta\nu_0$ (cm^{-1})
$W\,(3s\sigma)^1\Pi$ $v=0$	^{12}CO	102 806.74 (2)	1.5634 (5)	8.3 (2)$\times10^{-5}$		+0.3
	^{13}CO	102 775.71 (2)	1.5016 (46)(a)	9.6 (20)$\times10^{-5}$(a)		+1.6
$K\,(4p\sigma)^1\Sigma^+$ $v=0$(c)	^{12}CO	103 054.71 (2)	1.9159 (2)	5.85 (6)$\times10^{-5}$		+0.64
	^{13}CO	103 054.53 (4)	1.8174 (36)(a)	2 (1)$\times10^{-5}$(a)		+1.3
$L'\,(3d\pi)^1\Pi$ $v=1$	^{12}CO	103 211.88 (9)	1.7966 (23)(a)	1.0 (5)$\times10^{-5}$(a)		+0.7
$L\,(4p\pi)^1\Pi$ $v=0$	^{12}CO	103 271.87 (2)	1.959 68 (24)(b)	6.7 (1)$\times10^{-6}$(b)	0.0213 (12)(b)	+0.6
$(4d\sigma)^1\Sigma^+$ $v=0$	^{12}CO	105 676.51 (5)	1.8829 (21)(a)	1.0$\times10^{-5}$(a)		+1.0
$W\,(3s\sigma)^1\Pi$ $v=2$(c)	^{12}CO	106 250.81 (3)	1.6246 (8)	7.7 (8)$\times10^{-6}$(a)		+0.9
	^{13}CO	106 196.41 (5)	1.5370 (26)(a)	5 (3)$\times10^{-6}$(a)		+0.7
$^1\Pi$ $v=2$	^{12}CO	107 681.97 (4)	1.9118 (3)(a)	7.0$\times10^{-6}$(a)		+0.67
$^1\Sigma^+$ $v=2$	^{12}CO	109 448.97 (3)	1.7781 (7)	5.4 (1)$\times10^{-5}$(a)		+0.9
$(5p\sigma)^1\Sigma^+$ $v=1$	^{12}CO	109 481.03 (3)	1.829 (2)(a)	1.0$\times10^{-5}$(a)		+0.75

found, $\delta\nu_{obs}$ is 0.41 (5) cm^{-1} for $R(0)$ and 0.57 (7) cm^{-1} for $R(1)$. The spectrum of this band was of low intensity and only $R(0)$ and $R(1)$ states could be used for linewidth determination. For all other bands the values for the linewidths of unblended rotational lines were averaged, resulting in a reduced statistical uncertainty. The specific J-values that were included in the predissociation analysis for each particular vibronic state are listed in Table VIII.

IV. DISCUSSION AND CONCLUSIONS

Nine bands were measured in high resolution with a laser-based XUV spectrometer in the wavelength region 91–100 nm. Compared to recent experiments employing synchrotron radiation[3,4] or a large VUV-spectrograph[1,2] our instrumental resolution of 0.32 cm^{-1} is somewhat better. In several cases we were able to improve the accuracy of rotational constants but the major advantage of the present experiment lies in the capability of absolute calibration. As a consequence accurate values for the band origins could be derived. We estimate an absolute accuracy in the values for ν_0 of 0.13 cm^{-1}. The somewhat smaller values listed in Table VII stem from the internal consistencies of the fits.

The present values for ν_0 deviate substantially from those listed in the ^{12}CO atlas,[2] from 0.3 cm^{-1} for the $W\,^1\Pi$ $v=0$ state to 1.0 cm^{-1} for the $(4d\sigma)^+\Sigma^1$ $v=0$ state ($\delta\nu_0$ in Table VII). The shift in the band origin for ^{13}CO varies between 0.7 cm^{-1} [$W(3s\sigma)^1\Pi$ $v=2$] and 1.6 cm^{-1} [$W\,(3s\sigma)^1\Pi$ $v=0$]. Our accurate data have been used already for a recalibration of the CO-atlas in this wavelength region.[20]

There appears to be a systematic trend towards shorter lifetimes in the present data when compared with the values of Eidelsberg *et al.*[1] Particularly the $(5p\sigma)^1\Sigma^+$ $v=1$ and the $^1\Sigma^+$ $v=2$ states observed near 91.35 nm appear to dissociate an order of magnitude faster. An exception is formed by the $L\,(4p\pi)^1\Pi$ $v=0$ state where no broadening beyond instrumental width could be observed. A lower limit of $\tau > 3\times10^{-11}$ s may be estimated, a value in agreement with the value of Eidelsberg.[2] Some indication of isotopic dependent predissociation is found in the W $v=0$ state. In our previous paper we reported that the $^{13}C^{16}O$ isotope in the $v=2$ level of the same electronic state predissociates at a lower rate than the main isotope.[5] Different predissociation rates for the isotopic variations of CO may have some implications for the chemical modeling of inter-

TABLE VIII. Observed linewidth $\delta\nu_{obs}$, and deconvoluted values for the intrinsic linewidth Γ, excited state lifetime τ and predissociation rate k_p for several states of CO. Values for bands indicated with (c) were reported previously (Ref. 5); note that the present estimate differ somewhat from the preliminary estimates. In the last column the particular J-states used for the linewidth analysis are listed.

		$\delta\nu_{obs}$ (cm^{-1})	Γ (cm^{-1})	k_p (s^{-1})	τ (s)	τ (s), Ref. 2	J-states
$W\,(3s\sigma)^1\Pi$ $v=0$	^{12}CO	0.43 (7)	0.19 (10)	3.6 (19)$\times10^{10}$	2.8 (15)$\times10^{-11}$	10^{-10}	1–6,10,11
	^{13}CO	0.37 (5)		$<3\times10^{10}$	$>3\times10^{-11}$	10^{-10}	1,2
$K\,(4p\sigma)^1\Sigma^+$ $v=0$(c)	^{12}CO	0.40 (6)	0.14 (10)	2.7 (18)$\times10^{10}$	3.7 (25)$\times10^{-11}$	10^{-10}	0–3,5–12
	^{13}CO	0.40 (6)	0.14 (10)	2.7 (18)$\times10^{10}$	3.7 (25)$\times10^{-11}$	10^{-10}	1–4
$L'\,(3d\pi)^1\Pi$ $v=1$	^{12}CO	1.5 (5)	1.4 (5)	2.7 (9)$\times10^{11}$	3.7 (13)$\times10^{-12}$	3×10^{-12}	1
$L\,(4p\pi)^1\Pi$ $v=0$	^{12}CO	0.33 (8)		$<3\times10^{10}$	$>3\times10^{-11}$	10^{-10}	1,2
$(4d\sigma)^1\Sigma^+$ $v=0$	^{12}CO	1.0 (3)	0.90 (30)	1.7 (6)$\times10^{11}$	5.9 (20)$\times10^{-12}$	10^{-11}	1,2
$W\,(3s\sigma)^1\Pi$ $v=2$(c)	^{12}CO	0.7 (1)	0.55 (11)	1.0 (2)$\times10^{11}$	1.0 (2)$\times10^{-11}$	10^{-11}	1–4,7
	^{13}CO	0.47 (7)	0.25 (10)	4.7 (19)$\times10^{10}$	2.1 (9)$\times10^{-11}$	10^{-11}	1,2
$^1\Pi$ $v=2$	^{12}CO	0.49 (7)[a]	0.28 (9)	5.3 (17)$\times10^{10}$	1.9 (6)$\times10^{-11}$	10^{-11}	1,2
$^1\Sigma^+$, $v=2$	^{12}CO	0.7 (1)	0.55 (11)	1.0 (2)$\times10^{11}$	1.0 (2)$\times10^{-11}$	10^{-10}	0–2
$(5p\sigma)^1\Sigma^+$ $v=1$	^{12}CO	0.7 (1)	0.55 (11)	1.0 (2)$\times10^{11}$	1.0 (2)$\times10^{-11}$	10^{-10}	0–3

[a]Some indication of rotational dependence (see text).

stellar clouds. The error margins in the present values for predissociation rates are on the order of 20%–50%. In the near future we hope to improve our dye laser system resulting in a reduction of the spectral width of the XUV radiation by an order of magnitude. Our aim is to determine accurate lifetimes at the 3×10^{-10} s level and to study rotational-state-dependent predissociation effects.

In the range 91–100 nm eleven vibronic features could be observed with the technique of *1 XUV + 1 UV resonance ionization*, while in *absorption* 37 bands were observed.[2] However, the present experiments were performed on a molecular beam with orders of magnitude lower column density than in the measurements at the 10 m VUV spectrometer of Meudon. We estimate a pressure of 10^{-4} Torr and an efficient length of 1 cm in the interaction zone. A remarkable point is that some transitions, expected to be strong, were not observed. Because of the fast predissociation rates of the excited states of CO (Table VIII) the competition between predissociative decay and ionization is dominated by the first process. It has to be noted that the ionization is induced by a diverging UV laser beam. Under these circumtances the actual ionization rate is expected to be proportional to the excited state lifetime τ, as long as τ is shorter than the duration of the temporarily overlapped XUV/UV beams, which is 5 ns. In that case the signal intensities of individual lines in 1+1 resonance ionization is proportional to

$$I_{sig}\sim\sigma_{abs}\tau\sigma_{ion}\,. \tag{5}$$

Here σ_{abs} is the absorption cross section at maximum, and σ_{ion} is the UV-induced ionization cross section of the excited state. The dependency on the lifetime τ in Eq. (5) was found to be valid for 1+1 ionization processes in N_2 for predissociating states with lifetimes in the range 1.5–150 ps.[21] Despite a number of multiphoton ionization studies on CO (Refs. 9, 11, and 22) values for the ionization cross sections σ_{ion} for specific excited states of CO are not available. The following discussion is based on the assumption that σ_{ion} is constant for the states investigated. The maxima in the absorption cross section σ_{abs} may be adopted from Fig. 1 of Ref. 2 which represents a synthetic spectrum computed at 50 K based on experimentally deduced parameters. From a calculation of the product $\sigma_{abs}\tau$ it follows that the value for the K $(4p\sigma)^1\Sigma^+$ $v=0$ state and the L $(4p\pi)^1\Pi$ $v=0$ state are largest, 5.6×10^{-25} and 1.2×10^{-25} cm^2 s, respectively. Indeed these two states are observed in intense spectra. Based on such a calculation we can now understand why the L' $(3d\sigma)^1\Pi$ $v=1$ feature, clearly observable in absorption adjacent to the L $(4p\pi)^1\Pi$ $v=0$ band (see Fig. 1, Ref. 3) is barely visible in the present 1+1 ionization measurements. The lifetime of the L' state is estimated to be at least an order of magnitude shorter than that for the L state (see Table VIII), while its peak absorption is smaller by a factor of 2. In general we find that the observed relative band intensities of the 1 XUV+1 UV ionization spectra indeed scale with the calculated value for the product $\sigma_{abs}\tau$. However for a $5p\sigma$ $^1\Sigma^+$ $v=0$ feature at 93.31 nm the large value of 1.5×10^{-25} cm^2 s is calculated even if a low value for the lifetime of 10^{-11} s is taken (in Ref. 2 a value of 10^{-10} s is reported). Despite several efforts this vibronic feature could not be observed. We do not have an explanation for this fact other than pointing at the possibility of a reduced ionization cross section σ_{ion} in this energy window.

In the near future a monochromator setup to separate XUV and UV will be added to the XUV-laser spectrometer. The excited states, now investigated by 1 XUV+1 UV photoionization, can then be studied by straightforward XUV absorption. Values for photoabsorption cross sections may then be extracted directly from laser-based XUV studies. Comparing absorption spectra with 1 XUV+1 UV ionization spectra will then provide information on ionization cross sections as well.

ACKNOWLEDGMENTS

We thank Kjeld Eikema for his assistance during the measurements and their interpretation. Financial support from the Foundation for Fundamental Research on Matter (FOM) and the Netherlands Organization for the Advancement of Research (NWO) is gratefully acknowledged.

[1] M. Eidelsberg and F. Rostas, Astron. Astrophys. **235**, 472 (1990).
[2] M. Eidelsberg, J. J Benayoun, Y. Viala, and F. Rostas, Astron. Astrophys. Suppl. Ser. **90**, 231 (1991).
[3] K. Yoshino, G. Stark, P. L. Smith, W. H. Parkinson, and K. Ito, J. Phys. (Paris) Colloq. C1 **49**, 37 (1988).
[4] G. Stark, K. Yoshino, P. L. Smit, K. Ito, and W. H. Parkinson, Astrophys. J. **369**, 574 (1991).
[5] P. F. Levelt, W. Ubachs, and W. Hogervorst, J. Phys. II France **2**, 801 (1992).
[6] E. F. van Dishoeck and J. H. Black, Astrophys. J. **334**, 771 (1988).
[7] Y. P. Viala, C. Letzelter, M. Eidelsberg, and F. Rostas, Astron. Astrophys. **193**, 265 (1988).
[8] C. Letzelter, M. Eidelsberg, F. Rostas, J. Breton, and B. Thieblemont, Chem. Phys. **114**, 273 (1987).
[9] M. A. Hines, H. A. Michelsen, and R. N. Zare, J. Chem. Phys. **93**, 8557 (1990).
[10] P. Klopotek and C. R. Vidal, J. Opt. Soc. Am. B **2**, 869 (1985).
[11] N. Hosoi, T. Ebata, and M. Ito, J. Phys. Chem. **95**, 4183 (1991).
[12] S. Sekine, T. Masaki, Y. Adachi, and C. Hirose, J. Chem. Phys. **89**, 3951 (1988).
[13] S. Sekine, Y. Adachi, and C. Hirose, J. Chem. Phys. **90**, 5346 (1989).
[14] W.-Ü L. Tchang-Brillet, P. S. Julienne, J.-M. Robbe, C. Letzelter, and F. Rostas, J. Chem. Phys. **96**, 6735 (1992).
[15] P. F. Levelt and W. Ubachs, Chem. Phys. **163**, 263 (1992).
[16] S. Gerstenkorn and P. Luc, *Atlas du spectre d'absorption de la molecule de l'iode entre 14 800–20 000 cm^{-1}* (Editions du CNRS, Paris, 1978).
[17] S. Gerstenkorn and P. Luc, Rev. Phys. Appl. (Paris) **14**, 791 (1979).
[18] G. Guelachvili, D. de Villeneuve, R. Farrenq, W. Urban, and J. Verges, J. Mol. Spectrosc. **98**, 64 (1983).
[19] S. N. Dobryakov and Y. S. Lebedev, Sov. Phys. Dokl. **13**, 873 (1969).
[20] M. Eidelsberg, J. J. Benayoun, Y. Viala, F. Rostas, P. L. Smith, K. Yoshino, G. Stark, and C. A. Shettle (to be published).
[21] W. Ubachs, L. Tashiro, and R. N. Zare, Chem. Phys. **130**, 1 (1989).
[22] A. Fujii, T. Ebata, and M. Ito, Chem. Phys. Lett. **161**, 93 (1989).